

## On the Development of a Non-Equilibrium Diffusion Model

Bruno Baccus

*ISEN, 41 Boulevard Vauban, 59046 Lille Cedex, France*

Tetsunori Wada

*ULSI Research Center, Toshiba Corp.,  
1, Komukai Toshiba-Cho, Saiwai-ku, Kawasaki 210, Japan*

### Abstract

A new non-equilibrium diffusion model has been developed, and the following problems will be presented: the numerical solution, the determination of parameters values and the range of validity. Moreover, for the first time, transient-enhanced diffusion due to ion-implantation damage is successfully simulated in an unambiguous manner for both RTA and furnace annealing. Two-dimensional effects are also discussed.

In order to accurately simulate the formation of extremely shallow junctions, deep insight is needed into the physics of diffusion. In particular, transient-enhanced diffusion as a result of ion-implantation damage remains a difficult problem. From the modeling point of view, significant progress has been performed in the past [1] and most of the existing diffusion models assume equilibrium (except for bulk recombination). However, this is no more valid in the present case since the concentrations of the species including defects can exceed the dopant level [2]. Thus a complete non-equilibrium formulation is required. Such models have been already reported [3-4], but very few is known about their range of validity, prediction capabilities and the way to determine the involved parameters. This is the goal of this paper to present some answers to these questions, and to make comparisons with experiments using both RTA and furnace annealing.

### 1 The Model

Following previous works [3-4], it is considered that substitutional impurities are immobile and can diffuse only when paired with defects. In this kind of model, the possible reactions between the different species are always under non-equilibrium condition. Table I lists these reactions. This means that the diffusion of a dopant requires 5 coupled equations. However, it is needed to incorporate charged species to be able to simulate actual structures (bipolar profiles, for example). In order to limit the number of

unknowns, they are considered to be in equilibrium with the neutral ones: for interstitials and vacancies, Boltzmann statistics is used. It can be shown that charged impurity/point-defects pairs can also be expressed as a function of the neutral ones. Hence, the reactions in table I are generalized for each charged species. For example, if A is a donor, the continuity equation for (AV) pairs becomes, when including the electric field term:

$$\begin{aligned} \frac{\partial(AV)}{\partial t} &= \frac{\partial(AV)^0}{\partial t} + \frac{\partial(AV)^-}{\partial t} \\ &= \frac{\partial}{\partial x} \left[ D_{(AV)^0} \frac{\partial(AV)^0}{\partial x} + D_{(AV)^-} \frac{\partial(AV)^-}{\partial x} - \frac{q}{kT} D_{(AV)^-} (AV)^- \frac{\partial \Psi}{\partial x} \right] + (G - R)_{(AV)} \end{aligned} \quad (1)$$

where  $\Psi$  is the electrostatic potential. The last term in the right-hand side contains kinetic terms from the reactions described in table I. After expressing  $(AV)^-$  as a function of  $(AV)^0$  and introducing in (1), an effective diffusivity depending on electron concentration is obtained:

$$D_{(AV)}^{eff} = D_{(AV)^0} \left[ 1 + K \left( \frac{n}{n_i} \right) \frac{D_{(AV)^-}}{D_{(AV)^0}} \right] \quad (2)$$

where  $K$  depends on forward and reverse kinetic terms. The electron concentration  $n$  is calculated by solving Poisson equation. In short, this means that the present model has all the features of formulations like [5-6], but also includes the non-equilibrium conditions for all reactions.

## 2 Numerical Solution and Parameters Determination

### 2.1 Numerical solution

The resulting equations and algorithms have been implemented in the two-dimensional process simulator IMPACT4 [7], using the finite element method. As we need the same precision in defects and impurities description, the same mesh is always used for all the species. Concerning the time discretization, the implicit scheme together with an automatic time step selection such as proposed in [8] enables the time step to range from 0.1  $\mu$ s to several seconds in the case of annealing after ion implantation (section 4). On the other hand, a very high precision is required in the species concentrations, because of the kinetic terms. Hence, the stopping criterion for Newton-Raphson loops was defined as a relative change in concentrations less than  $5 \cdot 10^{-4}$ . In order to ensure numerical stability, mass-lumping was used for the temporal and kinetic terms. Finally, coupled and decoupled resolutions of the linear system have been compared. It was found that both methods converge towards the same results and moreover, the CPU time is comparable. This is a fortunate conclusion concerning the memory resource, since a coupled arsenic/boron diffusion needs 7 coupled equations for I, V, (As-I), (As-V), As, (BI), B. From the CPU time point of view, a factor between 100 and 500 is observed, compared to a standard steady-state model without point-defects [7].

## 2.2 Parameters values

One of the characteristics of such models is that they contain a large number of parameters, thus it is extremely important to describe the procedure for their extraction. Moreover, from a general point of view, it is of major interest to discuss the way to validate the obtained formulation.

All the parameters can be expressed as a function of a set of basic parameters, which are reported in table II. In particular, the kinetic terms are expressed as a function of  $R$ ,  $I^*$ ,  $V^*$  and the diffusivities of each species ( $D_I$ ,  $D_{(AI)}$ ...). As a result, the overall number of parameters to be fitted is significantly reduced. The procedure to determine their values is also explained in table II. In particular, the barrier energy for I-V recombinations  $\Delta E_{IV}$  was estimated at about 0.5 eV.

Once these parameters have been determined in the way presented above, they remain fixed for all the test examples reported in the following sections. Hence, all the forthcoming comparisons with experiments are done *after* extracting the parameters, or in other words, using *always* the same parameters values. This is in fact the only way to validate such type of model, otherwise the large number of involved parameters make possible the fit to almost any type of experiments, when using different values for each specific experiment.

## 3 Validity for Long and Short-Time Diffusion

In the case of high-concentration predeposition and compared to a standard model, if the same results are obtained for long-times, enhanced diffusion is observed for very short times (figure 1). This is due to the non-equilibrium treatment and it is confirmed by estimating non-equilibrium ratios as reported in figure 2. Such effects are significant only during a few seconds, afterwards equilibrium is reached (figure 2b). This kind of estimates could be also very useful to determine the time duration of the non-equilibrium regime, and then to use an equilibrium formulation such as [5-6,8].

The validity of the model for long-time diffusion is also confirmed in figure 3 which shows the effect of phosphorus diffusion on a boron buried layer. The phosphorus diffusion generates a supersaturation of interstitials which largely increases the boron diffusion [9]. It should be noted that if phosphorus is not present, boron displacement is very small. Here, it was found that the most important factor is the surface phosphorus concentration, because it controls the supersaturation of interstitials, via reactions (4-5) in table I.

## 4 Transient-Enhanced Diffusion due to Ion Implantation Damage

The model enable us to reproduce for the first time in an unambiguous manner the high activation energy of transient diffusion time (4.5 eV), reported from diffusion after low-dose boron implant [10]. Boron was implanted at an energy of 60 keV with a dose of  $2 \cdot 10^{14}$  at/cm<sup>2</sup>. The results are displayed in figure 4. The most important point here is that it shows that the model is continuous from RTA to furnace annealing conditions, without using some empirical factors (like time constants). Moreover, we have

studied the effect of the initial distribution of defects on transient diffusion. Simulations have been carried out for the three following cases: the initial distribution is 1) 4 times the dopant implanted profile, 2) 20 times the dopant profile, and 3) deduced from Monte Carlo calculations [11]. From figure 4, we conclude that it has a minor influence on the duration of transient diffusion. However, this is significant in terms of displacement (difference in boron profiles before and after diffusion, at a concentration level of  $10^{16}$  at/cm<sup>3</sup>), as illustrated in figure 5. Specifically, as the Monte Carlo simulation does not include self-annealing, initial defects concentrations are over-estimated and thus too much displacement is predicted in this case. The difference between experiments and simulations for low temperature is due to the clustering, which is not taken into account here, but which does not change the kinetic by itself. The same kind of calculation has been performed on bipolar devices and allows a deep understanding of damage effects on device performances [12].

Finally, the influence of ion-implantation damage on two-dimensional anomalous diffusion has been investigated. Boron was implanted at a dose and energy of  $4 \cdot 10^{13}$  at/cm<sup>2</sup> and 20 keV, and annealed at 800°C for 10 min. This is one of the cases where anomalous diffusion is the most remarkable. Figure 6 displays the boron contours at the end of the simulation. The maximum vertical displacement is on the order of 600 Å, whereas the lateral displacement is only about 320 Å. Hence, as in the case of predeposition [8], the surface effects limit the supersaturation of point-defects in the vicinity of the surface, and thus limit the amount of anomalous diffusion in the lateral direction.

## 5 Conclusions

In addition to a precise physical insight into the diffusion mechanisms, the detailed inclusion of point-defects under non-equilibrium condition allows to explain the effects of ion implantation damage on dopant diffusion. The generalization of this kind model seems very promising in order to investigate the problems arising in ULSI technologies.

## References

- [1] P. M. Fahey, P.B. Griffin and J.D. Plummer, *Reviews of Modern Physics*, vol. 61, No. 2, pp. 289-384, April 1989.
- [2] F.F. Morehead and R.F. Lever, *J. Appl. Phys.*, 66 (11), pp. 5349-5352, 1 December 1989.
- [3] T.L. Crandle, W.B. Richardson and B.J. Mulvaney, *IEDM Tech. Dig.*, pp. 636-639, December 1988.
- [4] M. Heinrich, M. Budil and H.W. Pötzl, *ESSDERC'90*, pp. 205-208, Eds W. Eccleston and P.J. Rosser, Nottingham, September 1990.
- [5] D. Mathiot and J.C. Pfister, *J. Appl. Phys.*, 55 (10), pp. 3518-3530, 15 May 1984.
- [6] M. Orlowski, *SISDEP III*, pp. 393-404, Eds G. Baccarani and M. Rudan, Bologna, September 1988.
- [7] B. Baccus, E. Dubois, D. Collard and D. Morel, *Solid-State Electron.*, vol. 32, No 11, pp. 1013-1023, November 1989.
- [8] E. Rorris, R.R. O'Brien, F.F. Morehead, R.F. Lever, J.P. Peng and G.R. Srinivasan, *IEEE Trans. Computer-Aided Design, CAD-9*, No 10, pp. 1113-1122, October 1990.

- [9] T.K. Okada, S. Kambayashi, S. Onga, I. Mizushima, K. Yamabe and J. Matsunaga, IEDM Tech. Dig., pp. 733-736, December 1990.
- [10] A.E. Michel, W. Rausch, P.A. Ronsheim and R.H. Kastl, Appl. Phys. Lett., 50 (7), pp. 416-418, 16 February 1987.
- [11] G. Hobler and S. Selberherr, IEEE Trans. Computer-Aided Design, CAD-7, No 2, pp. 174-180, February 1988.
- [12] B. Baccus, T. Wada, N. Shigyo, M. Norishima and H. Iwai, BCTM'91, Minneapolis, September 1991.

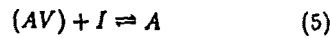
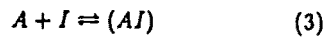
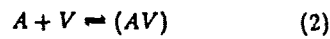


Table I: Reactions treated under non-equilibrium condition, where I, V, A, (AI) and (AV) refer to interstitials, vacancies, substitutional dopants, dopant-interstitial and dopant-vacancy pairs. For the sake of simplicity, only neutral species are reported here, but the model contains also charged species.

Parameter	Procedure/source
$R$	after Mathiot-Pfister
$I^*, D_I$	after Bronner
$V^*, D_V$	from thermodynamic
$E_{b(AV)}, E_{b(AI)}, D_{AV}, D_{AI}$	from predeposition calculations comparisons with standard steady-state models or experiments
$\Delta E_{IV}$	from high-concentration predeposition and diffusion after ion implantation

Table II: Determination of the basic parameters.  $R$  refers to the capture radius,  $E_{b(AX)}$  to the pairs binding energies and  $\Delta E_{IV}$  to the barrier energy for I-V recombination.

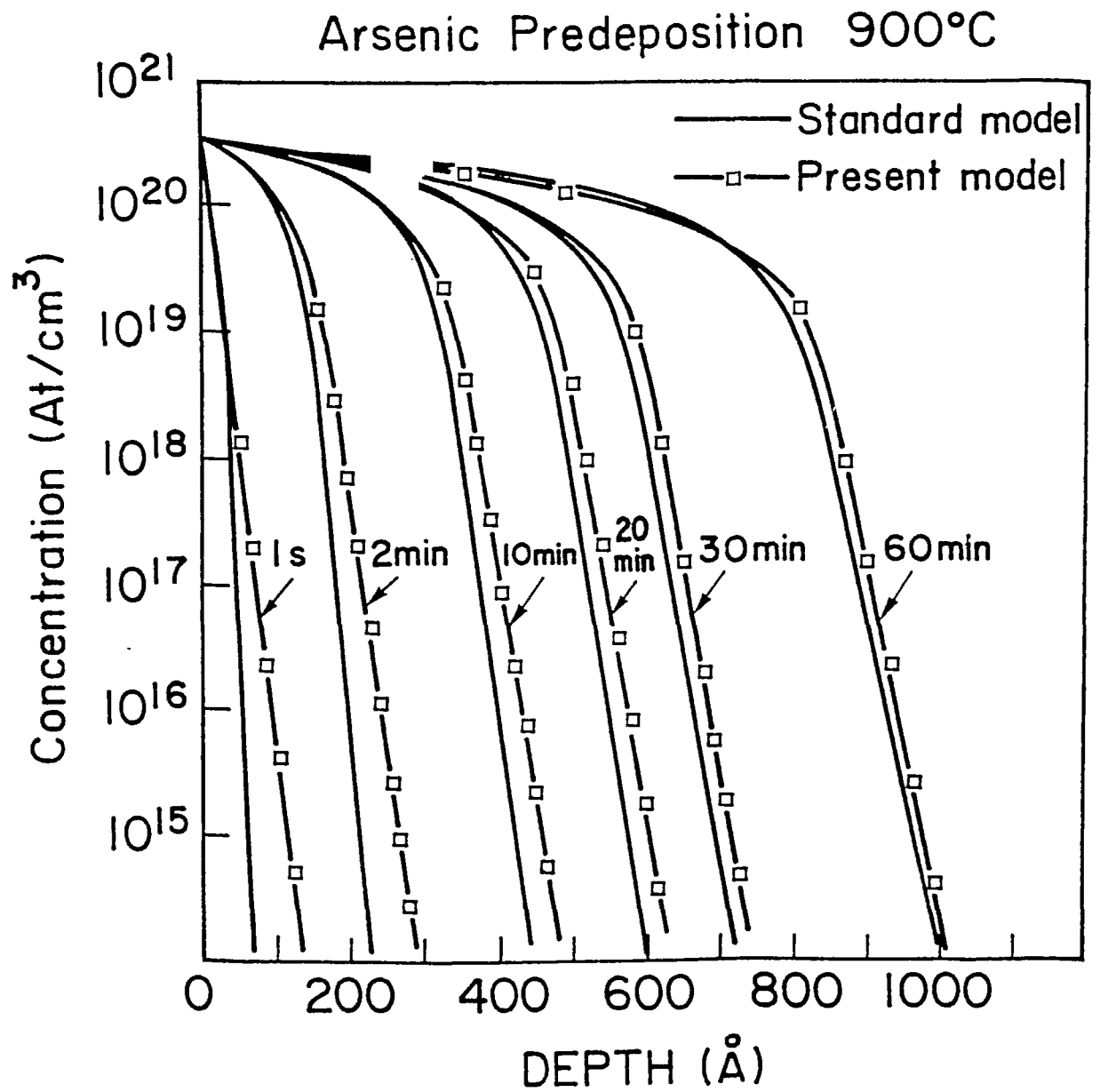


Figure 1: Arsenic predeposition at 900°C. Comparison between the new model and a standard one [7].

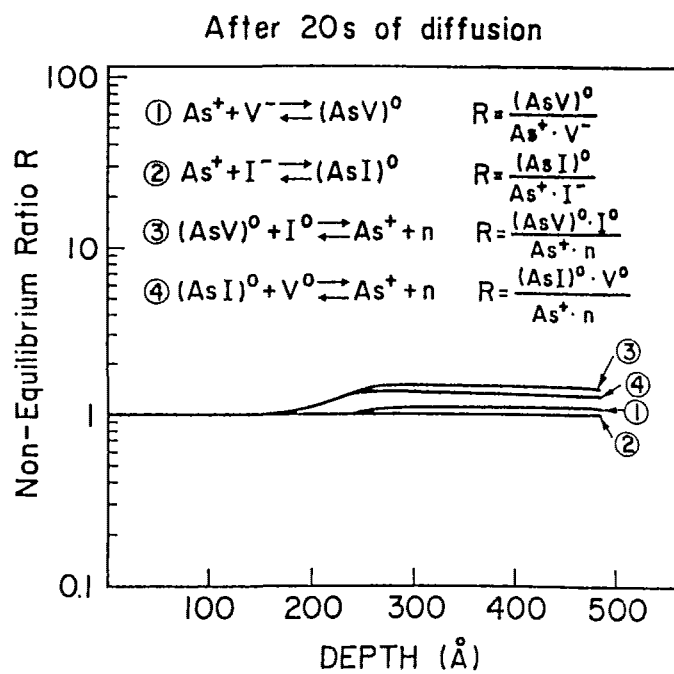
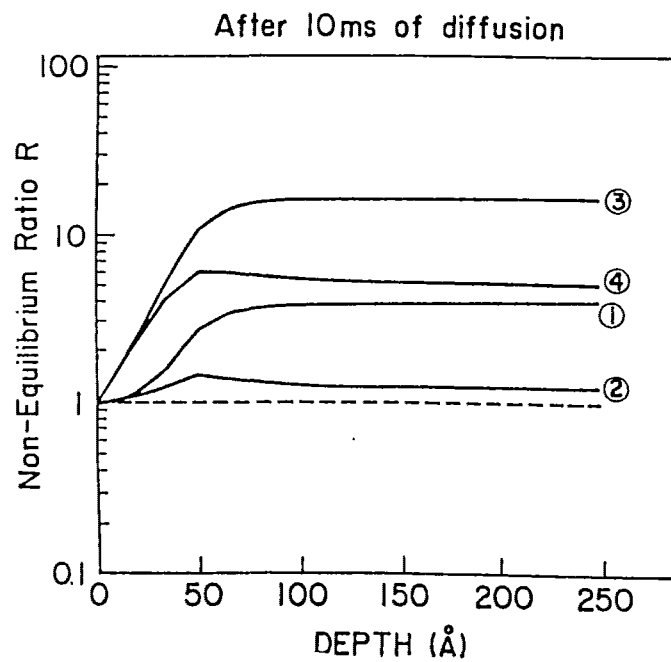


Figure 2: Evaluation of non-equilibrium ratios as a function of depth for the diffusion conditions from fig. 1.

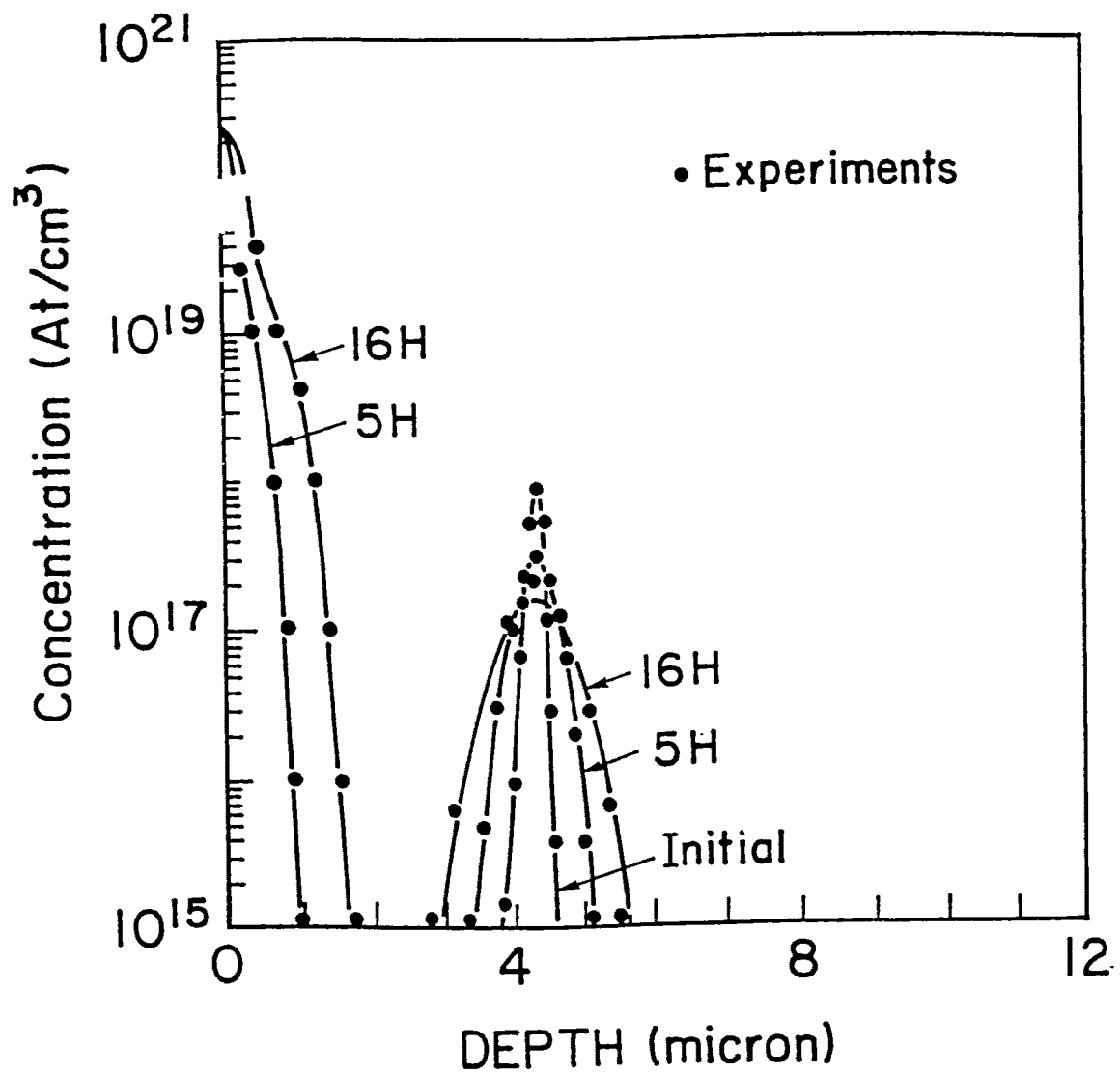


Figure 3: Comparison between experiments from [9] and simulation, for the diffusion from PSG film and the influence on a boron buried layer.

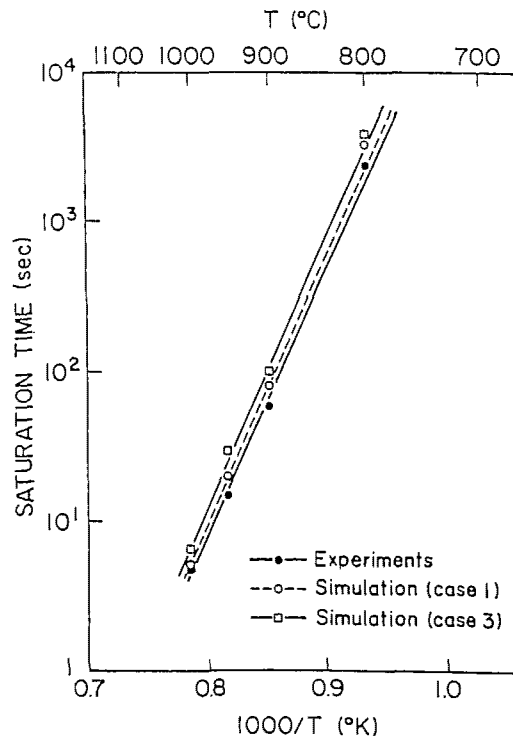


Figure 4: Transient-diffusion time after low-dose boron ion-implantation. Measurements are from [10]. The case 2 lies between cases 1 and 3.

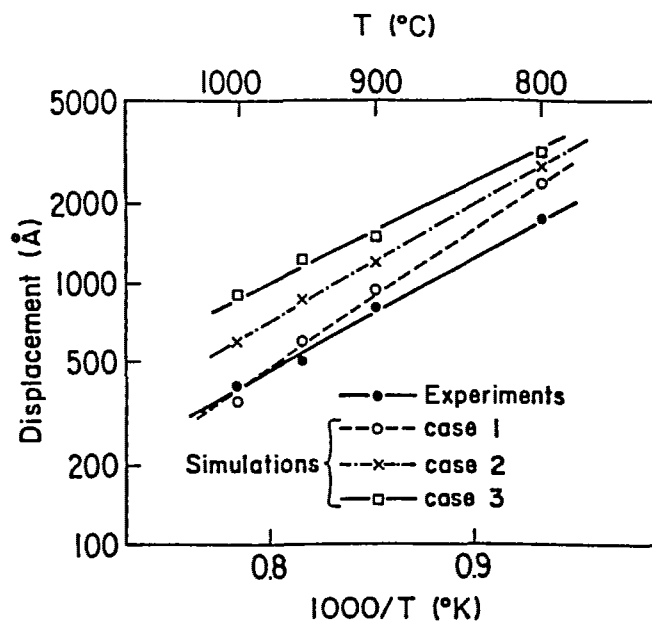


Figure 5: Boron displacement as a function of temperature. A standard model would predict no more than 100 Å.

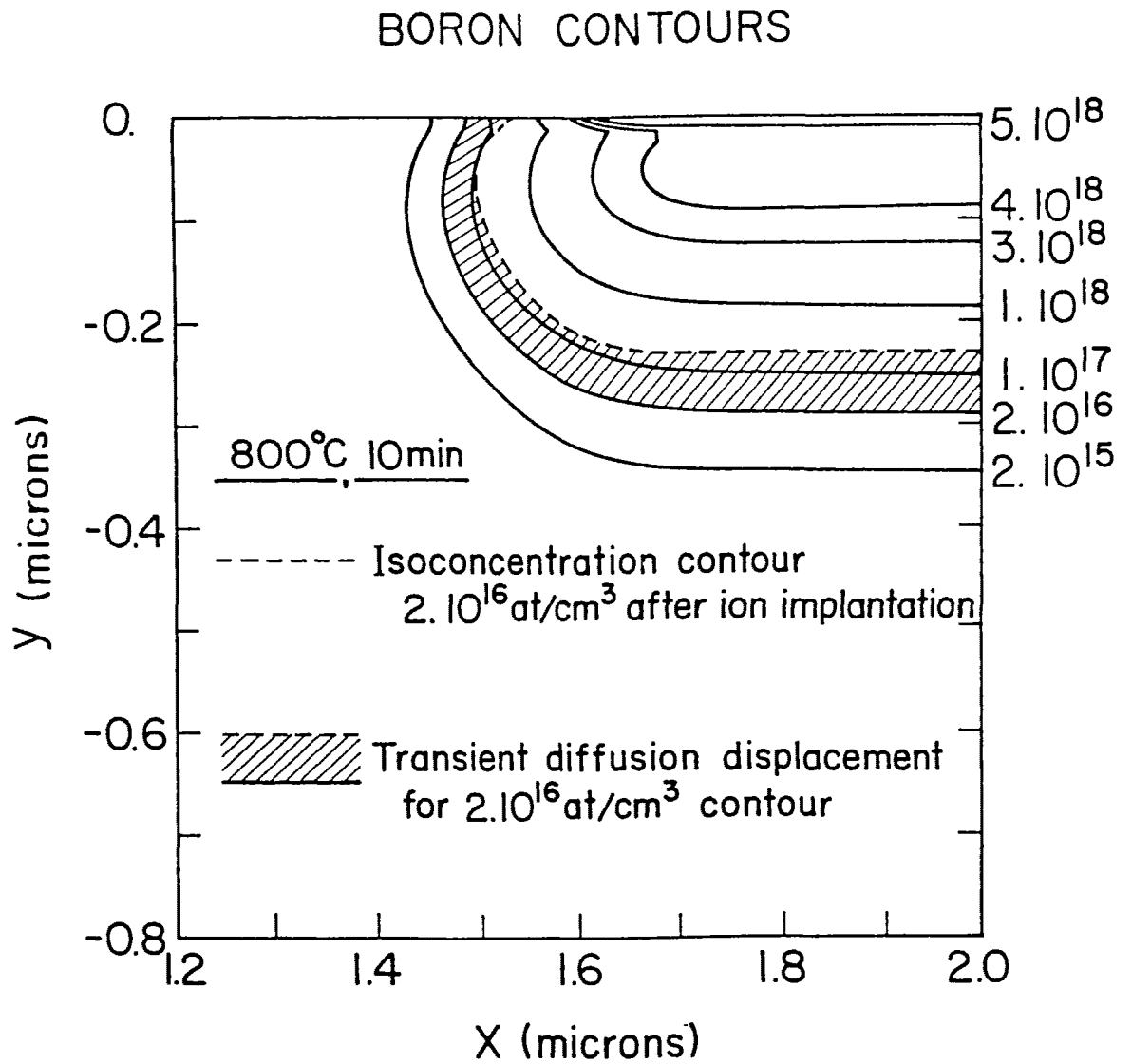


Figure 6: Boron contours showing the effect of ion-implantation damage on two-dimensional diffusion.